Journal of Molecular Liquids 211 (2015) 48–62

Contents lists available at ScienceDirect

Journal of Molecular Liquids

journal homepage: www.elsevier.com/locate/molliq

Role of surfactants on metal mediated cerium(IV) oxidation of valeraldehyde at room temperature and pressure

Aniruddha Ghosh, Pintu Sar, Susanta Malik, Bidyut Saha *

Homogeneous Catalysis Laboratory, Department of Chemistry, The University of Burdwan, Golapbag, Burdwan 713104, WB, India

ARTICLE INFO

Article history:
Received 16 March 2015
Received in revised form 16 June 2015
Accepted 18 June 2015
Available online xxxx

Keywords:
Valeraldehyde
Ce(IV)
Ir(III)
Valeric acid
CTAB

ABSTRACT

The short chain straight fatty acid, valeric or pentanoic acid is chemically significant for its huge applications in variety of industrial target compounds including plasticizers, lubricants, biodegradable solvents, perfumery and pharmaceuticals. Synthesis of valeric acid has been achieved by the cerium(IV) oxidation of a straight C_5 chain valeraldehyde which is a precursor of organic compounds. Ce(IV) is selected as an alternative oxidizing agent in place of higher valent metals. The oxidation kinetics of valeraldehyde has been investigated under pseudo-first-order conditions in acidic medium at 30 °C. Several transition metal salts: Cr(III), Mn(II), Cu(II), Ir(III) and Ru(III) have been introduced to observe their effect on reaction rate[6]. Three different representative non-functional surfactants: Cetyltrimethylammonium bromide (CTAB; cationic), Sodium dodecylsulphate (SDS; anionic) and 3-[(3-cholamidopropyl) dimethylammonio]-1-propanesulfonate (CHAPS; zwitterionic) catalyze the reaction significantly. Ir(III) and Ru(III) enhance the oxidation rate in the presence and absence of surfactant. Cr(III), Mn(II) and Cu(II) interestingly inhibit the reaction rate. CMC values of the surfactants have been determined by spectrofluorometry and conductometry. The oxidized product valeric acid has been characterized by NMR and FTIR spectroscopy. Scanning Electron Microscope (SEM) and Transmission Electron Microscope (TEM) experiments support the aggregation of surfactants Ru(III) in association with CTAB micellar catalyst that exhibited a dramatic ~330 fold rate enhancement compared to the uncatalyzed reaction path.

1. Introduction

Aldehydes are important trace constituents of the atmosphere. They have natural and anthropogenic sources, with small primary sources associated with vehicle exhaust and industrial activity and large secondary sources associated with the oxidation of volatile organic compounds [1,2]. Aldehyde oxidation is an important reaction for the manufacture of organic acids, peracids and anhydrides, which find applications as precursors for resins and pharmaceutical products [3]. Aliphatic aldehydes are extensively hydrated in aqueous solutions and many oxidation reactions proceed via the hydrate form [4]. The kinetics and oxidation mechanism of formaldehyde, acetaldehyde, propionaldehyde, and benzaldehyde in different media were studied.

n-Valeraldehyde, straight C_5 chain aldehyde, is used as an intermediate in the manufacture of alcohols, acids, esters, amines and other organic compounds [5,6]. n-Valeric acid (n-pentanoic acid) is the basis of new ester-type lubricants for CFC-substitutes in refrigeration systems which are made from the carboxylic acid with trimethylolpropane, pentaerythritol or dipentaerythritol. Valeric acid is prepared from butane cuts through hydroformylation to valeraldehyde with subsequent oxidation [7]. Industrially valeric acid is synthesized by Dow manufacture process by using the oxo process. Butylene is reacted with synthesis gas (carbon monoxide and hydrogen mixture) in the presence of a catalyst, yielding valeraldehyde. Valeraldehyde is then oxidized to valeric acid [6]. Valeric acid is mainly used as a chemical intermediate for the following compounds: Ester type lubricants, Flavors and perfumes, Plasticizers, Vinyl stabilizers, Specialty chemicals.

Regarding environmental problem and pollution, clean organic reaction processes which do not use the harmful organic solvents are encouraged and are in great demand today. Water as a cheap and relatively green solvent could be considered as an alternative reaction media for organic processes. The use of surfactants under micellar conditions represents one of the simplest methods to achieve catalysis in water since surfactants are in most cases very economical thanks to their extensive everyday use in detergency [8]. The contamination of aquatic environment by toxic metals, such as hexavalent chromium, lead, arsenic, cadmium is of great concern due to its trends to accumulate on vital organs of human and animals causing several health problems [9–12]. Therefore we have selected non toxic Ce(IV) as an alternating oxidizing agent in comparison to Cr(VI), Fe(VI), Pb(IV). The role of cerium as the most effective oxidant and catalyst in many organic syntheses is reflected in a number of reports in the literature. Cerium chemistry is dominated by the +3 and +4 oxidation states. The oxidative degradation of organic and inorganic compounds with cerium(IV) are potentially interesting, as cerium(IV) is an unusually strong, one-

* Corresponding author.
E-mail address: b_saha31@rediffmail.com (B. Saha).

http://dx.doi.org/10.1016/j.molliq.2015.06.056
0167-7322/

electron oxidant ($E^\circ = 1.4$ V in 1.0 mol dm^{-3} H_2SO_4) [13]. In sulfuric acid and sulfate media cerium(IV) forms several sulfate complexes. Generally transition metals in a higher oxidation state can be stabilized by chelation with suitable complex agent. However, our preliminary observations indicate that oxidation of some organic compounds by Ce(IV) in aqueous sulfuric acid is kinetically sluggish, the process can be efficiently catalyzed by various metal ions at trace concentration. Different metal ion catalysts like chromium(III), ruthenium(III), iridium(III) [14] etc. are generally used in the oxidation by cerium(IV). Among the different metal ions, ruthenium(III) [15] and iridium(III) [16] are highly efficient [17]. Reaction mechanism of various elementary reactions must be investigated to analyze the effect on selectivity. Therefore, the basic study of catalytic reaction will prove the scientific basis for improving catalyst selectivity and making high-efficiency catalyst. Various metal ions such as Ag(I), Mn(II), Cu(II), Os(VIII), Hg(II), Cr(III), Ru(III), Ir(III), etc. have been employed as catalysts in cerium(IV) oxidation of different types of substrates. However, ruthenium(III) and iridium(III) are highly efficient catalysts for cerium(IV) oxidations even at trace concentration levels (ca. 10^{-6}–10^{-7} mol dm^{-3}) [17,18].

The present work continues our kinetic studies of micellar effects on the metal-catalyzed oxidation of valeraldehyde. In this study, we have experimented with a nontoxic (benign) amphiphile (3-[(3-cholamidopropyl)dimethylammonio]-1-propanesulfonate (CHAPS)) in both water and metal-water media to look into their interactions to produce results that would lead to their uses in catalysis and industries. CHAPS is a zwitterionic derivative of cholic acid having combined properties of both sulfobetaine type detergents and bile salts [19]. Once again we have taken a more precise and detail experimental effort on the catalyzing properties of non-toxic surfactant CHAPS in oxidation kinetics [20].

Generally organic substrates are very often poorly soluble in water. Micellar systems can be used to overcome the solubility problems of the organic substrates. Self-organized assemblies such as micelles can change the rates of chemical and enzymatic reactions. Effects of micelles of surfactants on these reactions can be attributed to their electrostatic and hydrophobic interactions with reactants [21–23]. Surfactants are amphiphilic organic compounds, containing both hydrophobic groups and hydrophilic groups. Thus, a surfactant molecule contains both a water insoluble and a water soluble component [24]. We have employed an approach to the determination of kinetic constants of metal mediated-micelle catalyzed oxidation of valeraldehyde that allows the identification of important mechanism and function of different surfactants on the reaction rates. The different rate constants in the presence and absence of surfactants have been determined with the corresponding plots. SDS, CHAPS and CTAB have been found to accelerate the rate process for the valeraldehyde oxidation process.

2. Experimental

2.1. Materials and reagents

Valeraldehyde (SRL, AR, Mumbai, India), cerium(IV) ammonium sulfate (E. Merck, AR), cetyltrimethylammonium bromide (CTAB) (SRL, AR, Mumbai, India), CHAPS (SRL, AR, Mumbai, India), H_2SO_4 (E. Merck, AR), SDS (Qualizen) Na_2SO_4 (E. Merck, AR), HCl (E. Merck, AR), pyrene (SRL, AR, Mumbai, India), iridium(III) chloride (SRL, AR, Mumbai, India), ruthenium(III) chloride (SRL, AR, Mumbai, India), and all other chemicals used were of the highest purity available commercially. The stock solution of Ce(IV) was obtained by dissolving cerium(IV) ammonium sulfate in 1 mol dm^{-3} sulfuric acid and was standardized with iron(II) ammonium sulfate solution using ferroin as an external indicator [25,26]. Cerium(IV) solution was always made up and stored in a black coated flask to prevent photochemical reaction. A solution of iridium(III) chloride and ruthenium(III) chloride were prepared by dissolving the sample in a minimum amount of concentrated hydrochloric acid. The solution of surfactants were prepared by using the weighing balance (Sartorius BSA224S-CW) and dissolving calculated amount of surfactants in double distilled water through Digital Ultrasonic Cleaner CD 4820 instrument. Surfactant substrate mixture solution and other mixture solution containing surfactant were centrifuged to get a complete mixing through Centrifuge-Z206A (Hermle Labortechnik GmbH).

2.2. Kinetic measurements

Kinetic experiments were carried out spectrophotometrically by recording the changes in the Ce(IV) absorbance at 320 nm with a computer-controlled UV–VIS Shimadzu-1800 spectrophotometer, equipped with thermostated compartments for 1 cm cuvettes. The temperature of the experiments was regulated to 30.0 ± 0.1 °C with a thermostat TCC Shimadzu. The kinetics of the oxidation of the organic substrates by cerium(IV) were studied in the presence of a large excess of organic substrate over the Ce(IV) species: $[\text{valeraldehydel}]_T \geq 10[\text{Ce(IV)}]_T$. The observed pseudo-first-order rate constants, k_{obs}, were obtained from the slopes of the linear least-squares fit of the plot of $-\ln(A_{320})$ vs time (t) (Fig. 1), and were reproducible to within 3% with good correlation coefficient values [16,20,25,26]. The kinetics was followed up to 80% completion of the reaction and good first-order kinetics were observed. The $t_{1/2}$ values are directly calculated in Table 1 by using the relation $t_{1/2} = (\ln 2/k_{obs})$, where ln2 = 0.693, k_{obs} = pseudo-first-order rate constant in s^{-1}. The k_{obs} values were found to be independent of the initial Ce(IV) concentration, and consequently, the oxidation rates are first order with respect to the oxidizing species. The surfactant concentrations used in all experiments were notably above the critical micelle concentrations [27,28] to make sure of the existence of micellar aggregates in the solution. The possibility of decomposition of the surfactants SDS, CTAB and CHAPS by Ce(IV) has been investigated and the rate of decomposition has been found negligible [29].

2.3. Product analysis and stoichiometry

Ce(IV) (2.0×10^{-4} mol dm^{-3}) was taken in distilled water (15 ml) and H_2SO_4 (4.2 ml). A solution of substrate (2.0×10^{-3} mol dm^{-3}) was added to the reaction mixture and stirred for 24 h at 30–35 °C. Ether was added to the reaction mixture. The organic layer was extracted, washed with water, and dried over anhydrous $MgSO_4$. Ether was removed by warming, and the products [4] were obtained (valeric acid from valeraldehyde), whose boiling points were in agreement with literature values (yields ~85–90%). The reaction product was subjected to FTIR (Fig. S1, Supplementary material) (Shimadzu Prestige-21) and proton NMR analysis, and characterized as follows: Valeric acid: υ = 2958 (br, s, −OH), 2673, 1705 (s, C═O), 1411, 1211, 937, 748 cm^{-1}.

The oxidation products were analyzed by the ^1H NMR with a Bruker ASCEND spectrometer at a frequency of 400 MHz using $CDCl_3$ as the solvent and $SiMe_4$ as internal standard (Fig. S2, Supplementary material) [30].

The stoichiometry of the reaction in the case of valeraldehyde may be given by Eq. (1):

$$2\text{Ce(IV)} + C_4H_9CHO + H_2SO_4 \rightarrow 2\text{Ce(III)} + C_4H_9COOH + 2H^+. \quad (1)$$

2.4. Test for free radicals

Acrylonitrile (monomer) was used for the identification of free radicals. In a typical experiment, reaction mixture containing $[\text{Ce(IV)}] = 2.0 \times 10^{-4}$ mol dm^{-3}, $[\text{valeraldehyde}] = 2.0 \times 10^{-3}$ mol dm^{-3}, $[H_2SO_4] = 0.5$ mol dm^{-3}, and acrylonitrile (=30% v/v) at 30 °C led to the formation of white polymeric product indicating in situ generation of free radicals [13,25].

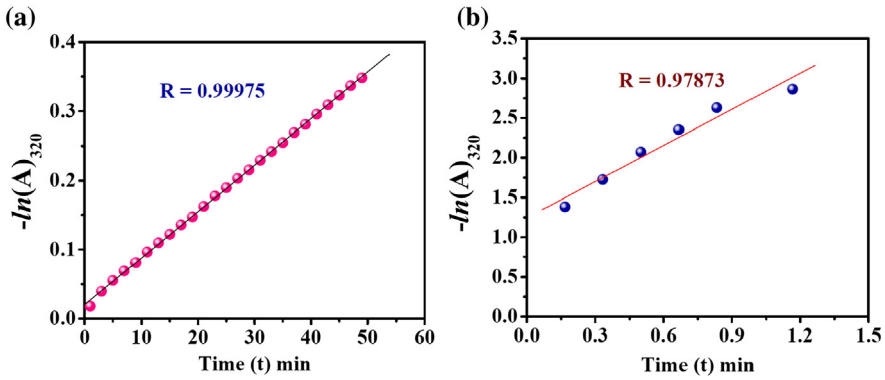

Fig. 1. Representative first-order plot for Ce(IV) oxidation of valeraldehyde in uncatalyzed and Ru(III) mediated CHAPS catalyzed path. $[Ce(IV)]_T = 2 \times 10^{-4}$ mol dm^{-3}, $[H_2SO_4]_T =$ 0.5 mol dm^{-3}, $\mu = [H_2SO_4 + Na_2SO_4] = 2.0$ mol dm^{-3}, $[valeraldehyde]_T = 2 \times 10^{-3}$ mol dm^{-3},Temp = 30 °C. (a) $[Ru(III)]_T = 0$ mol dm^{-3}, $[CHAPS]_T = 8 \times 10^{-3}$ mol dm^{-3}; (b) $[Ru(III)]_T = 6 \times 10^{-4}$ mol dm^{-3} $[CHAPS]_T = 10 \times 10^{-3}$ mol dm^{-3}.

Table 1
Effect of the different surfactants, Ir(III) and Ru(III) catalyst on pseudo-first order rate constant and half-life for the Ce(IV) oxidation of valeraldehyde.

Substrate	$[H^+]$ (mol dm^{-3})	$10^6 \times$ metal catalyst (mol dm^{-3})		$10^3 \times$ micellar catalyst (mol dm^{-3})		$10^4 \times k_{obs}$ (s^{-1})	Half life ($t_{1/2}$) (h)
Valeraldehyde	0.5	–		–		1.121 ± 0.02	1.71
	1.0					1.26 ± 0.03	1.527
	1.5					1.6383 ± 0.05	1.175
	2.0					1.683 ± 0.07	1.143
	2.5					2.183 ± 0.05	0.87
	0.5	Cr(III)	2	–	–	0.763 ± 0.09	2.523
		Mn(II)	2			0.966 ± 0.05	2.0
		Cu(II)	2			0.898 ± 0.08	2.14
	0.5	Ir(III)	2	–	–	2.3283 ± 0.02	0.826
			3			2.515 ± 0.04	0.826
			4			2.8316 ± 0.06	0.68
			5			3.0616 ± 0.02	0.628
			6			3.425 ± 0.03	0.56
	0.5	Ru(III)	2			60.3 ± 0.05	0.032
			3			125.4 ± 0.03	0.0153
			4			172.2 ± 0.06	0.011
			5			190.3 ± 0.03	0.0101
			6			203.8 ± 0.04	0.0094
	0.5	–		SDS	10	2.112 ± 0.03	0.91
					12	2.483 ± 0.06	0.77
					14	2.955 ± 0.03	0.65
					16	3.125 ± 0.05	0.616
					18	3.269 ± 0.03	0.588
	0.5	–		CTAB	1.5	1.3966 ± 0.03	1.378
					2.0	1.228 ± 0.04	1.567
					2.5	1.167 ± 0.07	1.65
					3.0	1.071 ± 0.04	1.79
					3.5	0.6916 ± 0.06	2.783
	0.5	–		CHAPS	10	1.225 ± 0.03	1.57
	0.5	Ir(III)	2	SDS	10	3.766 ± 0.02	0.51
				CTAB	1.5	2.995 ± 0.05	0.64
				CHAPS	10	14.4 ± 0.06	0.133
	0.5	Ru(III)	2	SDS	10	25.6 ± 0.04	0.0752
				CTAB	1.5	80.8 ± 0.04	0.0238
				CHAPS	10	78.7 ± 0.06	0.0244
	0.5	Ir(III)	6	SDS	10	10.2 ± 0.02	0.188
				CTAB	1.5	8.037 ± 0.02	0.24
				CHAPS	10	55.7 ± 0.03	0.034 (Time of completion)
	0.5	Ru(III)	6	SDS	10	147.2 ± 0.03	2.354 min
				CTAB	1.5	365.3 ± 0.02	56.9 s.
				CHAPS	10	264.8 ± 0.03	1.30 min

$[Ce(IV)]_T = 2 \times 10^{-4}$ mol dm^{-3}, $[Valeraldehyde]_T = 2 \times 10^{-3}$ mol dm^{-3}, $\mu = 2.0$ mol dm^{-3}, Temp = 30 °C.

Fig. 2. Spectral changes observed during the course of the uncatalyzed and metal mediated micelle catalyzed oxidation of valeraldehyde by Ce(IV) in sulfuric acid media. Experimental conditions: $[Ce(IV)]_T = 2.0 \times 10^{-4}$ mol dm^{-3}, $[valeraldehyde]_T = 2.0 \times 10^{-3}$ mol dm^{-3} $[H_2SO_4]_T = 0.5$ mol dm^{-3}, $\mu = 2.0$ mol dm^{-3}, Temp = 30 °C. (a) [catalyst] = 0 mol dm^{-3}, time interval = 2 min; (b) $[CHAPS]_T = 10.0 \times 10^{-3}$ mol dm^{-3}, time interval = 1 min; (c) $[CTAB]_T = 1.5 \times 10^{-3}$ mol dm^{-3}, Time interval = 1 min; (d) $[SDS]_T = 10.0 \times 10^{-3}$ mol dm^{-3}, time interval = 1 min; (e) $[Ir(III)]_T = 6.0 \times 10^{-4}$ mol dm^{-3}, [surfactant]$_T$ = 0 mol dm^{-3},time interval = 1 min; (f) $[Ru(III)]_T = 2.0 \times 10^{-4}$ mol dm^{-3}, [surfactant]$_T$ = 0 mol dm^{-3}, time interval = 1 min; (g) $[CTAB]_T = 1.5 \times 10^{-3}$ mol dm^{-3}, $[Ir(III)]_T = 6.0 \times 10^{-4}$ mol dm^{-3}, time interval = 15 s; (h) $[CTAB]_T = 1.5 \times 10^{-3}$ mol dm^{-3}, $[Ru(III)]_T = 6.0 \times 10^{-4}$ mol dm^{-3}, time interval = 15 s.

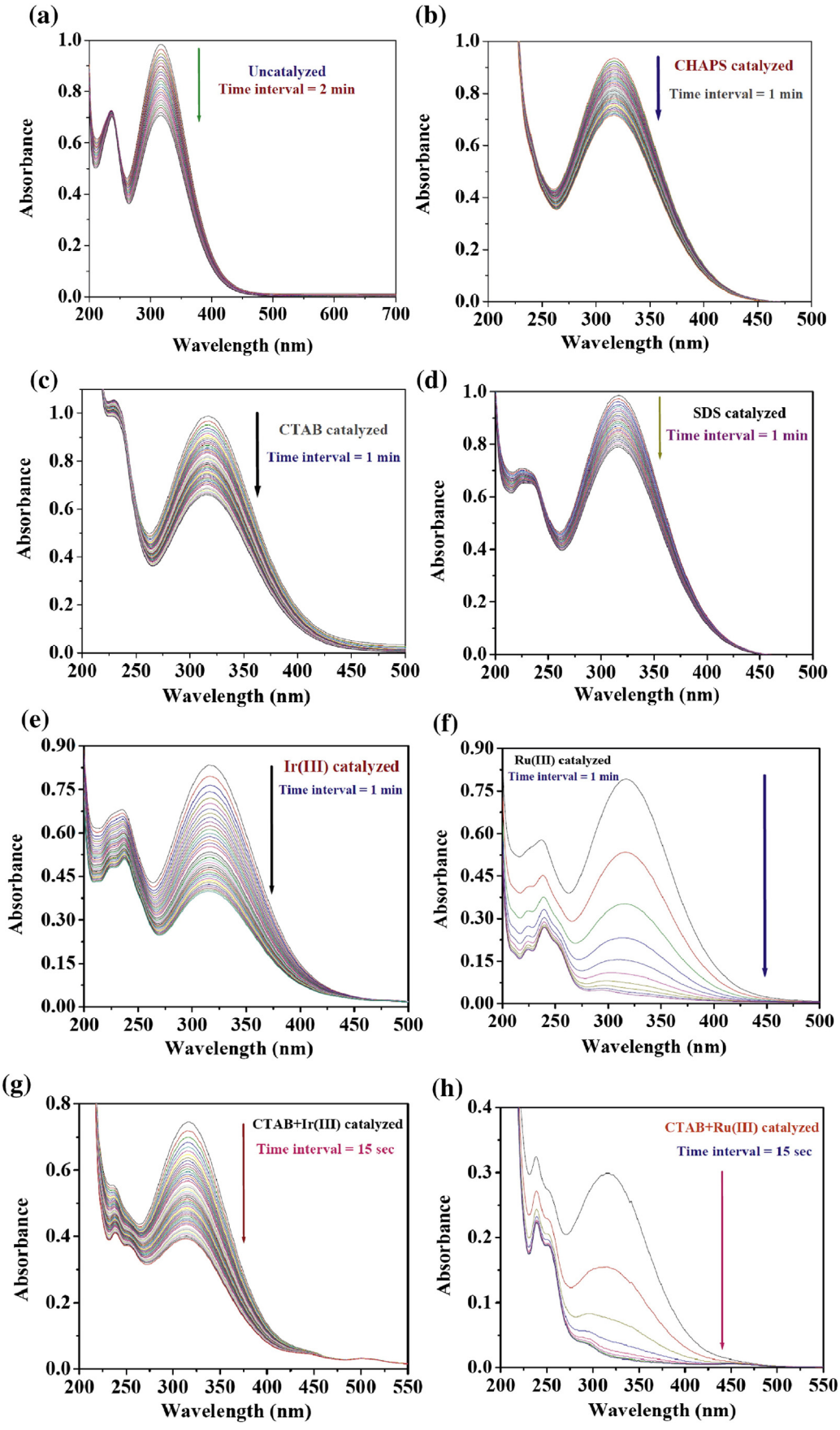
(a)
Uncatalyzed
Time interval = 2 min
Absorbance
Wavelength (nm)
(b)
CHAPS catalyzed
Time interval = 1 min
Absorbance
Wavelength (nm)
(c)
CTAB catalyzed
Time interval = 1 min
Absorbance
Wavelength (nm)
(d)
SDS catalyzed
Time interval = 1 min
Absorbance
Wavelength (nm)
(e)
Ir(III) catalyzed
Time interval = 1 min
Absorbance
Wavelength (nm)
(f)
Ru(III) catalyzed
Time interval = 1 min
Absorbance
Wavelength (nm)
(g)
CTAB+Ir(III) catalyzed
Time interval = 15 sec
Absorbance
Wavelength (nm)
(h)
CTAB+Ru(III) catalyzed
Time interval = 15 sec
Absorbance
Wavelength (nm)

2.5. Critical micelle concentration (CMC) measurement

2.5.1. Fluorimetry

Fluorescence measurements were performed in a spectrofluorometer (Hitachi) using a quartz cell of path length 1 cm at 30 ± 0.1 °C temperature with excitation and emission slit width of 3.0 nm and 2.5 nm respectively and scan speed 500 nm min^{-1}. Pyrene was used as the fluorescence probe. A series of surfactant solutions were prepared for fluorescence intensities measurement following the procedure used in spectrophotometry. The solutions were excited at 334 nm, and the emission spectra were recorded in the range 360–450 nm. The fluorescence intensities of the peaks at ~372 nm (I_1) and ~383 (I_3) were extracted from the spectra, and the I_3/I_1 value vs. surfactant CHAPS concentration was used for CMC determination. The CMC was found around 6.3 mM from the plot of fluorescence intensity versus CHAPS concentration (Fig. S3a, Supplementary material).

2.5.2. Conductometry

The CMC values of SDS and CTAB was obtained by using conductometric method with the help of a water analyzer kit (Eutech instrument, Cyber Scan 6000 Series Meters). Conductance values were plotted against concentration of SDS (Fig. S3b, Supplementary material) and CTAB (Fig. 4a, Supplementary material). CMC value obtained from the plots were 8.2 mM for SDS and 1.1 mM for CTAB [31,32]. The critical micelle concentration (CMC) of CTAB in presence of valeraldehyde was also determined from the break points of nearly two straight-line portions of the specific conductivity versus concentration plot. The CMC value of CTAB was found to be 1.02 mM by conductometry in presence of valeraldehyde (2.0×10^{-3} mM) (Fig. 4b, Supplementary material).

3. Results

3.1. UV–VIS spectrophotometric study of the reaction

UV–vis spectroscopy is a well-known technique for monitoring the completeness of reaction. Indeed, solutions of ceric salts are yellow or deep orange-red in the presence of valeraldehyde, whereas solutions of cerous salts are colorless. Fig. 2 shows the UV–vis spectra recorded within certain time up to the completion of the reaction at room temperature. A continuous color change of the solution with time is observed as Ce^{4+} is converted into Ce^{3+} [33].

The reaction mixture were scanned in the range 200–700 nm in both presence and absence of the metal ion [Ir(III) and Ru(III)] individually at regular time intervals to follow the gradual development of the reaction intermediates (if any) and the end product. The presence of Ce(IV) ion can generate charge transfer bands which are also related to the color mechanism, giving in this case a yellow coloration. Ce(IV) favors charge transfer (CT) transitions from the host ligands to the rare earth ions. In the case of cerium, 4f–5d bands of Ce^{3+} ions and the CT bands of Ce^{4+} ions appear in the same wavelength range (Fig. 2a–h), which cause them to overlap each other [34,35]. The scanned absorption spectra of the different set of reaction mixtures were taken for both in presence and absence of surfactant and metal ion catalyst Ir(III)/Ru(III) (Fig. 2). Replicate scans of the spectra during the course of the reaction showed a decrease in the absorbance only, with no evidence of any shift in the peaks (Fig. 2). Spectroscopic test was carried out by comparing the electronic spectrum of the reaction mixture one minute after the start of the reaction with that of the final product within a wavelength of 200–700 nm.

The absorbance maximum at 320 nm due to the electronic transitions of the cerium(IV) complexes. The color of Ce(IV) compounds in aqueous medium is due to the LMCT bands. The absorption spectrum of Ce(IV) species in aqueous sulfuric acid solution differs from that of Ce(III) species [20]. The UV–VIS spectral band of valeraldehyde-cerium(IV) mixtures observed at 320 and 223 nm are the evidence of complex formation between them (Fig. 3a). However, Ce(III) complexes produced after completion of reaction have an absorption band near 250 nm (Fig. 3b). The reason for these changes is the disappearance of the intensive yellow colored cerium(IV), which is reduced to a pale green cerium(III). In the presence and absence of both Ir(III) and Ru(III), the cerium(III) complexes produced after completion of reaction in this work, are practically transparent in visible spectral region and exhibit only less intensive absorption bands at 295, 254, 241, 223 and 212 nm respectively in UV region (Fig. 3b). In contrast, with cerium(III) the lowest energy electronic absorption bands in the UV regions corresponding to the $4f^n \rightarrow 4f^{n-1}d^1$ transition. The electronic spectrum of Ce(III) consists of a single transition between $^2F_{5/2}$ (ground state) and $^2F_{7/2}$.

3.1.1. Spectral evidence for metal–substrate complex formation

The experimental results indicate that formation of a complex between valeraldehyde with iridium(III) and ruthenium(III). The spectral evidence for the formation of a complex between the substrate and catalyst was obtained from UV–Vis spectra of valeraldehyde-iridium(III) and valeraldehyde–ruthenium(III) mixtures. The experimental result suggest that valeraldehyde combines with the active species of the catalyst to form a complex, which then reacts in a slow step with 1 mol of cerium(IV) to give the product cerium(III). The spectral evidence for a complex between substrate and catalyst is obtained from UV–VIS spectra (Fig. 4) of only Ir(III) and Ru(III) solutions followed by valeraldehyde-metal catalyst mixtures in which there were changes in the band was observed. The spectra obtained for the metal–substrate mixture were different and significant new peak appeared at 295 nm.

The band observed for free Ir(III) solution at 488 nm, 433 nm and 229 nm respectively and Ru(III) solution in the region of 455 nm, 357 nm and 257 nm respectively (Fig. 4) which remain almost identical with the band appeared after completion of the reaction for both Ir(III) and Ru(III) mediated reactions. It is quite significant that after completion of Ir(III) and Ru(III)-metal mediated reactions the metals bring back to its previous oxidation state. From which anyone can definitely conclude that both of these metal act as catalyst in the oxidation process.

3.2. Dependence on [H_2SO_4]

The reaction was carried out at various initial concentration of sulfuric acid at a fixed valeraldehyde concentration as in Table 1. It was observed that the rate of oxidation reaction increased with increasing sulfuric acid concentration. The plots of k_{obs} versus [H^+] (Fig. 5) for the oxidation of valeraldehyde are found to be linear in nature with good correlation coefficient of 0.96917. This indicates that the reaction order with respect to [H^+] is first. Since the rate increases with increasing hydrogen ion concentration (Table 1), Ce^{4+} should be more reactive species in the form of sulfato–Ce(IV) complexes [25]. On the basis of rate acceleration effects of H_2SO_4, the $Ce(SO_4)^{2+}$ has been considered to be the reactive form in most of the reactions of cerium(IV) [20].

The kinetics of the oxidation of valeraldehyde by cerium(IV) in the absence and presence of surfactants was investigated under varying conditions of [metal catalyst], [H_2SO_4].

3.3. Dependence on Ir(III)

Plots of k_{obs} versus [$IrCl_3$] gave straight lines passing through the origin for valeraldehyde, indicating that the reaction follows first-order kinetics with respect to iridium(III) chloride concentrations [16]. Addition of traces of Ir(III) significantly enhances the rate. Pseudo-first order rate constant k_{obs} vs. [Ir(III)] yielded good linear plot (Fig. 6a and Table 1). Rate values increase proportionately with increasing [Ir(III)] and in that case reaction follows first order kinetics with respect to iridium(III) chloride concentrations. Recently, similar behavior has been reported in the oxidation of some aromatic aldehydes by Ce(IV) in the presence of iridium(III) chloride [34,36].

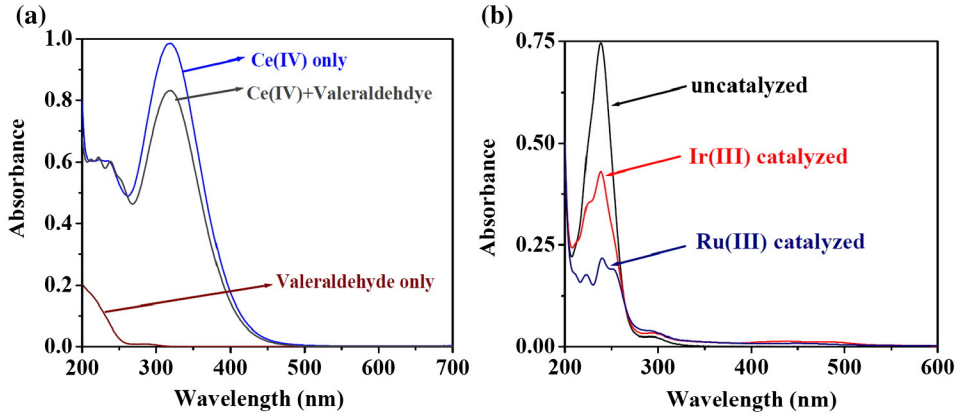

Fig. 3. Absorption spectra of Ce(IV) solutions along with Ce(IV)-valeraldehyde mixtures and Ce(III) solution produced after completion of the uncatalyzed and metal catalyzed reaction at 30 °C. $[Ce(IV)]_T = 2 \times 10^{-4}$ mol dm^{-3}, $[H_2SO_4]_T = 0.5$ mol dm^{-3}, $\mu = 2.0$ mol dm^{-3}, (a) $[valeraldehyde]_T = 2.0 \times 10^{-3}$ mol dm^{-3}; $[Ce(IV)]_T = 2 \times 10^{-4}$ mol dm^{-3}, (b) $[valeraldehyde]_T = 2.0 \times 10^{-3}$ mol dm^{-3}; (uncatalyzed) → $[metal\ catalyst]_T = 0$ mol dm^{-3}, (Ir(III)-catalyzed) → $[Ir(III)]_T = 6.0 \times 10^{-4}$ mol dm^{-3}, (Ru(III)-catalyzed) → $[Ru(III)]_T = 6.0 \times 10^{-4}$ mol dm^{-3}.

3.4. Dependence on Ru(III)

The fact that under the experimental conditions in the absence of Ru(III) ions the reaction practically does take place at a moderate rate [37] supported by an independent experiment. Addition of traces of Ru(III) enhances the rate significantly (Fig. 6b and Table 1). The concentration of ruthenium(III) chloride was varied from (2.0–6.0) × 10^{-6} mol dm^{-3}. The rate increases with increasing of ruthenium(III) chloride. On plotting the k_{obs} values versus [Ru(III)], rate values increase proportionately with increasing [Ru(III)] and yields a almost linear plot (Fig. 6b). The experimental rate constant value increased with Ru(III) concentration both in presence and absence of surfactants SDS, CTAB and CHAPS. The rate data for the Ru(III) mediated path in presence of SDS, CTAB and CHAPS surfactant at constant concentration have been calculated at 6.0 × 10^{-6} mol dm^{-3} concentration of Ru(III). The kinetic data for the higher concentration of Ru(III) (6.0 × 10^{-6} mol dm^{-3}) have been calculated and found that Ru(III) assist the oxidation reaction to undergo complete about just 1–2 min (Table 1).

3.5. Dependence on surfactant concentration

In our study of micellar rate effects, CTAB is found to increase. Attraction and repulsion, respectively, between the positively charged Ce(IV) species and the head groups of three types of surfactant micelles seemingly play important role in the present case. The rate of conversion increased with an increase in the surfactant concentration higher than CMC, and leveled off after the surfactant concentration reached 2CMC. Therefore, at high CTAB concentration, the rate of reaction increase gradually but it will be slowed down at 3.5 mM and the conversion of valeraldehyde did not change significantly [38]. Cetyltrimethylammonium bromide (CTAB, a representative cationic surfactant) is found to accelerate valeraldehyde oxidation path. Plots of $k_{obs(T)}$ versus $[CTAB]_T$ (cf. Fig. 7a, Table 1) shows a slight increase and finally it tends to level off at higher concentration of CTAB. With the increase of SDS concentration the rate constant increased even after reaching CMC (Fig. 7b, Table 1).

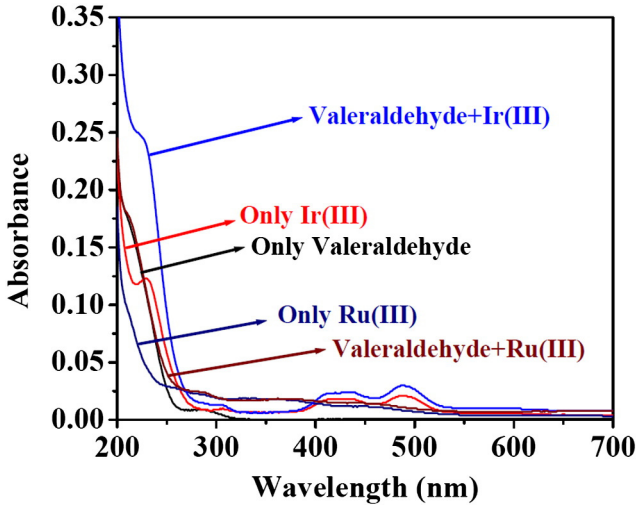

Fig. 4. Absorption spectrum of only Ir(III) and Ru(III) solutions (without substrate and oxidant) in aqueous medium and absorption spectrum of reaction mixtures with Ir(III) and Ru(III) solution (without oxidant): $[Ir(III)]_T = 6.0 \times 10^{-4}$ mol dm^{-3}, $[Ru(III)]_T = 6.0 \times 10^{-4}$ mol dm^{-3}; $[valeraldehyde]_T = 2.0 \times 10^{-3}$ mol dm^{-3}, $[Ir(III)]_T = 2 \times 10^{-6}$ mol dm^{-3}; $[valeraldehyde]_T = 2.0 \times 10^{-3}$ mol dm^{-3}, $[Ru(III)]_T = 6.0 \times 10^{-4}$ mol dm^{-3}, temp = 30 °C.

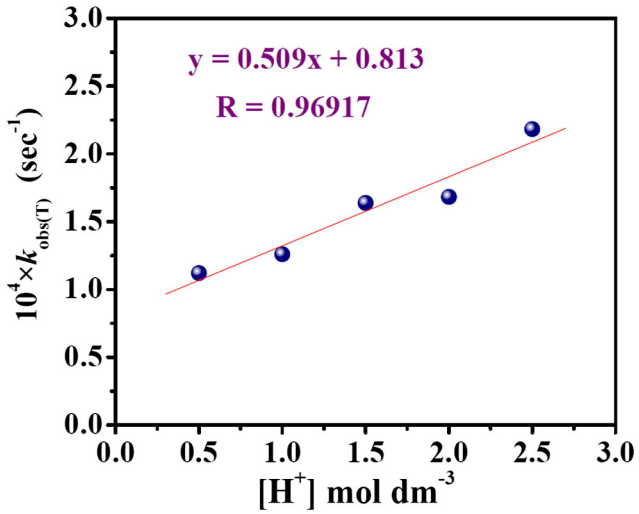

Fig. 5. Dependence of k_{obs} on $[H^+]$ for the Ce(IV) oxidation of valeraldehyde at 30 °C. $[Ce(VI)]_T = 2 \times 10^{-4}$ mol dm^{-3}, $[valeraldehyde]_T = 2 \times 10^{-3}$ mol dm^{-3}.

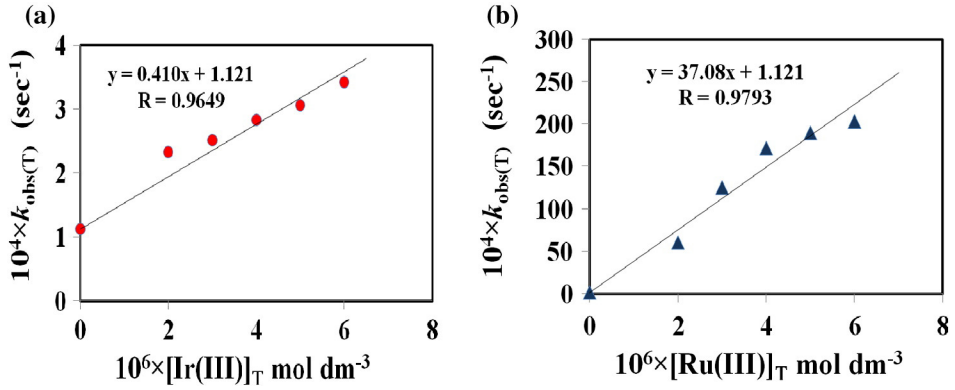

Fig. 6. Dependence of $k_{obs(T)}$ on [metal catalyst] for the Cr(VI) oxidation valeraldehyde in the absence of surfactant in aqueous H_2SO_4 media at 30 °C. $[Ce(VI)]_T = 2 \times 10^{-4}$ mol dm^{-3}, $[valeraldehyde]_T = 2 \times 10^{-3}$ mol dm^{-3}, $[H_2SO_4]_T = 0.5$ mol dm^{-3}, $\mu = 2.0$ mol dm^{-3}, temp = 30 °C. (a) for Ir(III) mediated; (b) for Ru(III) mediated.

3.6. High resolution transmission electron microscope (HRTEM) images of micelles

The HR-TEM investigation was done on JEOL JEM 2100 microscope operating at 20 KV acceleration voltage using lacey carbon coated Cu grid of 300 mess size. Samples were prepared by placing sample mixture drops directly on the copper grids using a micropipette. The surfactants present in the aqueous solution were allowed to settle. TEM pictures (Fig. 8) are presented which illustrate the multiple morphologies of the aggregates made from the surfactants. Also, the micrograph suggests a relatively narrow size distribution of the cylindrical micelle diameters, but a widely variable length. Transmission electron micrographs of CHAPS micelles are mainly observed spherical large unilamellar vesicles (Fig. 8a). In the corresponding TEM image, globular and near globular type particles of varied sizes were observed. The TEM display looked like disintegrated/disaggregated isolated bodies. In the corresponding TEM images of CTAB, loosely arranged ensembles of small to large globular and near globular particles forming spherical entities were observed (Fig. 8b). At [SDS] > CMC_e, broken rock-type materials of large size appeared in the TEM picture (Fig. 8c). With the addition of reactants (valeraldehyde), the morphology changes at some extent may be due to the accumulation valeraldehyde at the aqueous micellar surface. Cylindrical vesicles were converted to the spherical micelles in presence of valeraldehyde as depicted in the images (Fig. 8d and f). The effect of concentration is extremely important since possible aggregates are initially typically spherical micelles, but as soon as the concentration increases also ellipsoidal micelles, rods, hexagonal liquid crystal phase (LC, hexagonal arrangement of long cylinders), lamellar LC phase and, eventually, reverse phases are possible [8].

4. Discussion

4.1. Reaction mechanism of uncatalyzed path

The presence of electron-releasing groups (R = C_4H_9) accelerated the oxidation process by increasing the electron availability at the oxygen of the aldehydic carbonyl group. This facilitated the attack of the electrophile $[Ce(SO_4)^{2+}]$ [4]. This mechanism involves the initial complex formation between the organic substrate and the reactive cerium(IV) species. Subsequently, the intermediate complex decomposes in the rate-determining electron-transfer step, yielding a free carbon radical and the cerium(III) species. The final reaction products are obtained by the subsequent fast oxidation of the organic radical. This type of mechanism has been proposed previously [17,34,39] the oxidation of a variety of organic substrates by cerium(IV) in sulfuric acidic media. The kinetics of the forgoing reactions were studied and showed that substrates and oxidant interact in an equilibrium step to form an intermediate complex which is assumed to disproportionate forming a free radical and reduced Ce(IV). On the basis of above statement and observed first order dependence on [oxidant] as well as [substrate] a probable mechanism is proposed for the oxidation of valeraldehyde such complex formation between the oxidant and substrate was observed in earlier studies [20,34,40,41]. Thus a mechanism consistent with the above kinetics is proposed (Scheme 1).

4.2. Mechanism of Ir(III)-catalyzed path

It is known that $IrCl_3$ in hydrochloric acid gives $IrCl_6^{3-}$ species. It has also been reported that iridium(III) and iridium(I) ions are the stable

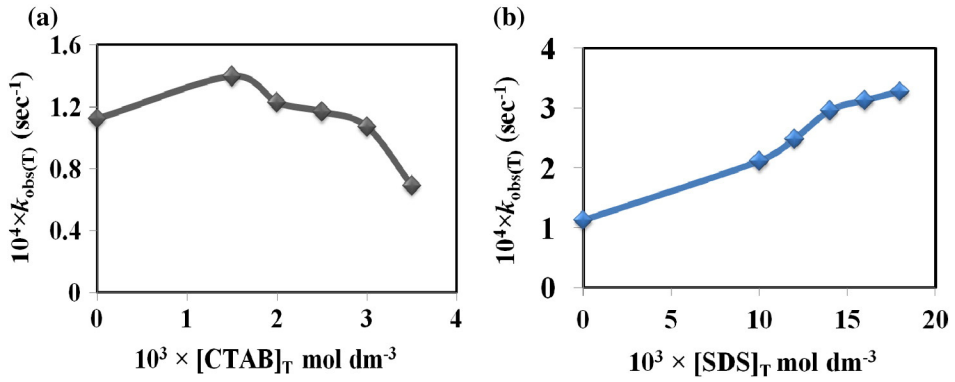

Fig. 7. Influence of the surfactants on the k_{obs} for the Ce(IV) oxidation of valeraldehyde in aqueous H_2SO_4 media at 30 °C. $[Ce(VI)]_T = 2 \times 10^{-4}$ mol dm^{-3}, $[valeraldehyde]_T = 2 \times 10^{-3}$ mol dm^{-3}, $[H_2SO_4]_T = 0.5$ mol dm^{-3}, $\mu = 2.0$ mol dm^{-3}. (a) For CTAB; (b) for SDS.

species of iridium. Further, the aquation of $[IrCl_6]^{3-}$ gives $[IrCl_5(H_2O)]^{2-}$, $[IrCl_4(H_2O)_2]^{-}$ and $[IrCl_3(H_2O)_3]$. Considering our experimental results, $IrCl_6^{3-}$ is likely to be the reactive species of iridium(III) chloride in the present study, which has also been considered previously [42]. The possibility of association of valeraldehyde and Ce(IV) ($\mathbf{C_1}$) leading to certain interaction between valeraldehyde and Ce(IV) in the first equilibrium step (Scheme 2), was detected by UV–vis absorption spectra of valeraldehyde-Ce(IV) mixture solutions. Spectral evidence suggesting that 1:1 type complex formation between valeraldehyde and Ir(III) in the second equilibrium step. The second equilibrium probably involves the outer-sphere association ($\mathbf{C_1}$) of the valeraldehyde and Ir(III) catalyst followed by the electron transfer leading to the complex ($\mathbf{C_2}$) which may be (valeraldehyde)·Ir(III), subsequently electron transfer occurs within the complex to give Ir(III) and the free radical which is rapidly oxidized by Ce(IV) at a fast step. [16].

4.3. Mechanism of Ru(III)-catalyzed path

A variety of ruthenium complexes are found to be active catalysts for the oxidation of various organic compounds, using terminal oxidants such as Ce(IV), hydrogen peroxide, O_2, or periodate [43]. The proposed mechanism involves the formation of a 1:1 complex between Ru(III) and valeraldehyde, which then reacts with Ce(IV). The results of the kinetic studies indicate that valeraldehyde may be involved in complex formation either with Ru(III) or Ce(IV). The evidence of Ru(III)-substrate complex has been confirmed by the shift in the absorption maximum of Ru(III) from 230 nm to 290 nm. Further, formation of higher oxidation states of Ru(III) has been reported earlier [34,44]. If the formation of the Ru(III)-substrate adduct is taken as the first step, the reaction mechanism could be written as in Scheme 3.

The rate of the reaction has not affected much with Cu^{2+}, Mn^{2+} and Cr^{3+} hence cannot show any catalytic activity in this reaction. But these metals have catalytic activities on different substrates as reported previously [40].

4.4. Structures of different surfactants

Micellar catalysis critically depends on the interactions of the micelle with the substrate(s) and the activated complex. This is an extremely complicated problem because a number of different interactions are involved including those associated with the head group of the surfactant, different segments of the alkyl chain and the counter ions [29].

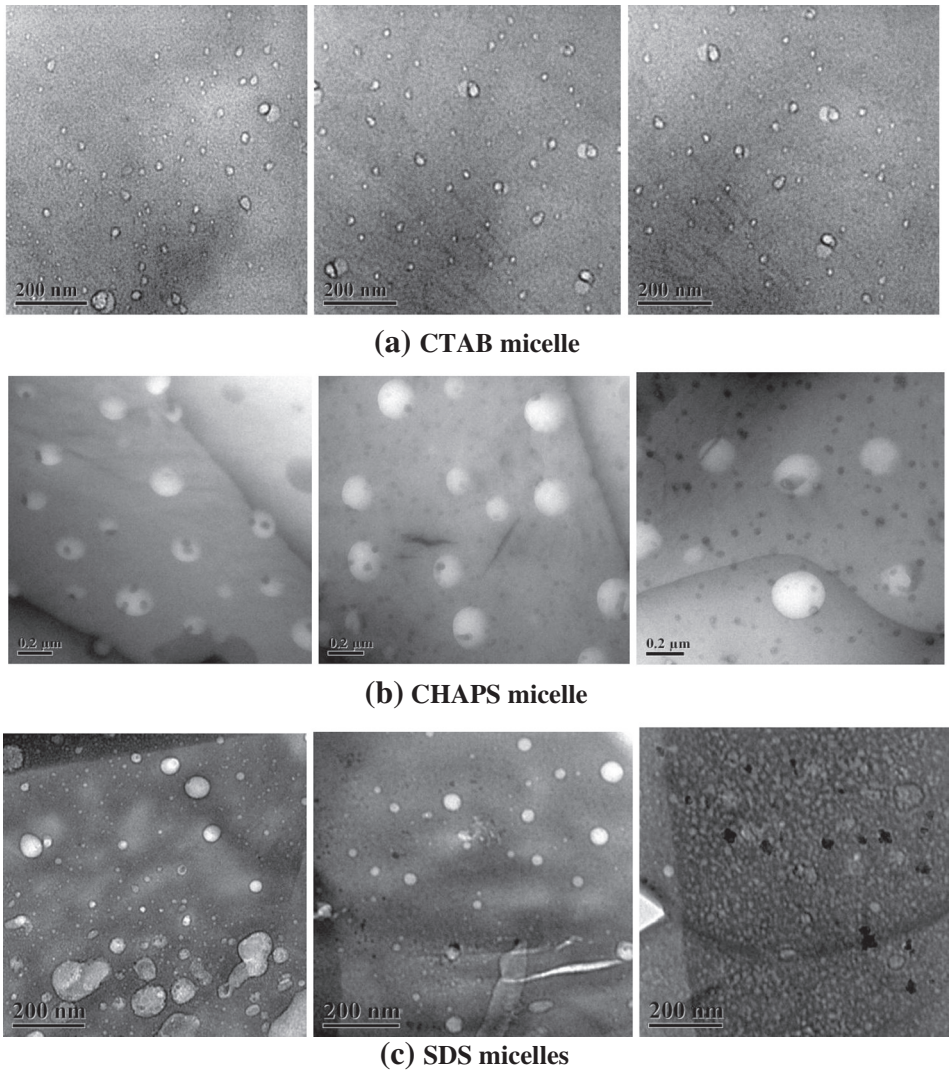

Fig. 8. (a) to (c): Different views of TEM images showing micelles formed by CTAB, CHAPS and SDS surfactants in aqueous medium at 30 °C. [CHAPS] = 10.0×10^{-3} mol dm^{-3}, [CTAB] = 1.5×10^{-3} mol dm^{-3}, [SDS] = 10×10^{-3} mol dm^{-3}. (d) to (f) Different views of TEM images of the surfactant–substrate mixture showing the interaction of valeraldehyde with surfactant micelles in aqueous medium at 30 °C. $[CTAB]_T = 1.5 \times 10^{-3}$ mol dm^{-3}, $[CHAPS]_T = 10.0 \times 10^{-3}$ mol dm^{-3}, $[SDS]_T = 10.0 \times 10^{-3}$ mol dm^{-3}, $[valeraldehyde]_T = 2.0 \times 10^{-3}$ mol dm^{-3}.

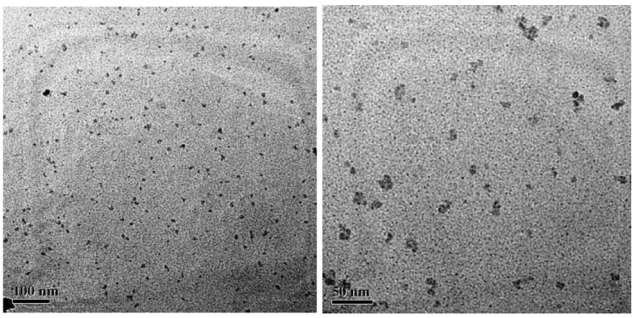

(d) CTAB micelles in presence of valeraldehyde

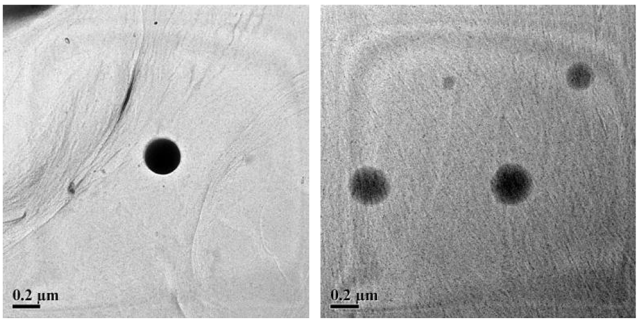

(e) CHAPS micelles in presence of valeraldehyde

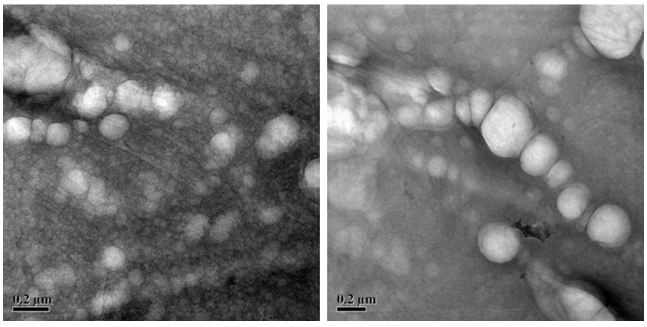

(f) SDS micelles in presence of valeraldehyde

Fig. 8 (*continued*).

4.5. Micellar effect on reaction rate

An analysis of the reaction medium properties of the stern region is of wide interest because the majority of reactants used in organic reactions in micellar solutions bind in the micellar Stern region [20,21,31,45]. The increasing interest over the past several decades in organic reactivity in aqueous solutions has resulted in widespread use of micelles to increase the solubility of hydrophobic compounds in aqueous solutions [46,47]. A characteristic feature of the stern region of ionic micelles (SDS, CHAPS and CTAB) (Fig. 9a to c) is the high local concentration of headgroups, counterions, and backfolding surfactant tails residing at the micelle interface. It can be concluded that a better description of micellar effects on the reaction rates includes the contribution of hydrophobic interactions with the backfolding hydrocarbon tails. The local negative charge in the Stern region of anionic SDS and zwitterionic CHAPS micelles has a stabilizing effect on the partial positive charge developing in the intermediate complex (Scheme 4a to d). The combined effect of the electrostatic neutrality in the micellar interfacial region on the transition state and specific interactions with surfactant head groups explains why the micellar rate constants for SDS, CHAPS and CTAB micelles (Table 1) are greater by a factor of ca. 2 to 3 than that in aqueous medium only. In this micellar catalysis reaction, micelles solubilize the organic reactant valeraldehyde and the catalyst, placing them in close proximity inside the small volume of the micellar pseudophase [48].

Addition of increasing amounts of the cationic surfactant CTAB has little inhibitory influence on the redox process with Ce(IV) and valeraldehyde (Fig. 7a and Table 1). In the presence of the anionic surfactant SDS at the concentration above CMC (equal to the highest [CTAB] used), a increaser in the rate constant can be observed. The observed surfactant effects on the redox reactions can be qualitatively interpreted by the pseudophase model, bearing in mind that, in the presence of cationic CTAB micelles, hydrophilic positively charged ions [H^+, and cationic reactive cerium(IV) species] will compete for binding to the micelle by exchanging the bound (bromide) counterions, while anionic species [HSO_4^-, SO_4^{2-}, and anionic reactive cerium(IV) species are very unlikely at the acid concentration used in this work] will be confined to the intermicellar aqueous phase. The converse will occur with the anionic SDS and zwitterionic CHAPS micelles.

4.5.1. Effect of SDS on enhancement of reaction rate

Specific hydrogen ion involved oxidations are accelerated by anionic micelles, as in the case of our study, sodium dodecyl sulfate, SDS, and increased the rates as the substrate and H^+ became micellar bound and then went through maxima due to competition between H^+ and Na which was used in much of this early work [21–23,27,28,49]. The dependence of first-order rate constants on [surfactant] is typically governed by partitioning of the substrate between water and micelles (Scheme 4a and b). In case of SDS, there is a attraction between the anionic head group ($-OSO_3^-$) and the reactive cerium (IV) species (positively charged) may form an ion-pair. Thus, an increase in the effective concentration of cerium(IV) within a small volume takes place. In addition, the partitioning of valeraldehyde in the micellar pseudophase cannot be ruled out because the stern layer is water rich (the water activity in the aqueous phase and in the micellar pseudophase is similar [50].

4.5.2. Influence of CHAPS on enhancement of reaction rate

The surfactant CHAPS also has the ability of being able to incorporate a large number of reactants and substrate molecules well into its small volume of surface. The incorporation of the reactants and substrate molecules into the CHAPS micelles could affect the physical properties of the micelle in two ways. The first is to reduce the overall net negative and positive charge on the surface of the micelle, thus reducing the strength of the electrostatic interaction between the oxidant and metal–substrate complex with the micelle. The second is to reduce the packing density of the micelle. Thus, overall increment of rate occurs due to the increased concentration of both valeraldehyde and $Ce(SO_4)^{2+}$-Ir(III)/Ru(III)-complex in the stern layer (Scheme 4c and d) of micelle [20]. Thus, 3-[(3-cholamidopropyl) dimethylammonio]-1-propanesulfonate, better known as CHAPS behaves differently from the normal charged surfactants because of the presence of OH groups in the CHAPS molecule, possibly interacts with the valeraldehyde molecule through conformation changes of the amphiphile.

The oxidation reaction rates observed (Table 1) in CHAPS micellar media can be differentiated from those observed in conventional media. This is accounted for the solubilization as well as orientation of the reactants, reduction of their effective concentrations through their segregation in different 'compartments' within the bulk medium. The faster oxidation rate is attributed to the higher reactant concentration within CHAPS micelles, the changes in the polarity and physicochemical properties of the medium [51,52]. The zwitterionic micellar surface of CHAPS attracts the cationic species $Ce(SO_4)^{2+}$ and metal-valeraldehyde positive complex due to electrostatic or coulombic interactions. Again the hydrophobic interactions can bring about the incorporation of the reactants (substrate) into micelles. Thus, overall increment of rate occurs due to the increased concentration of both valeraldehyde and $Ce(SO_4)^{2+}$/metal-complex in the Stern layer (Scheme 4c and d) of micelle. Based on electrostatic [20] considerations,

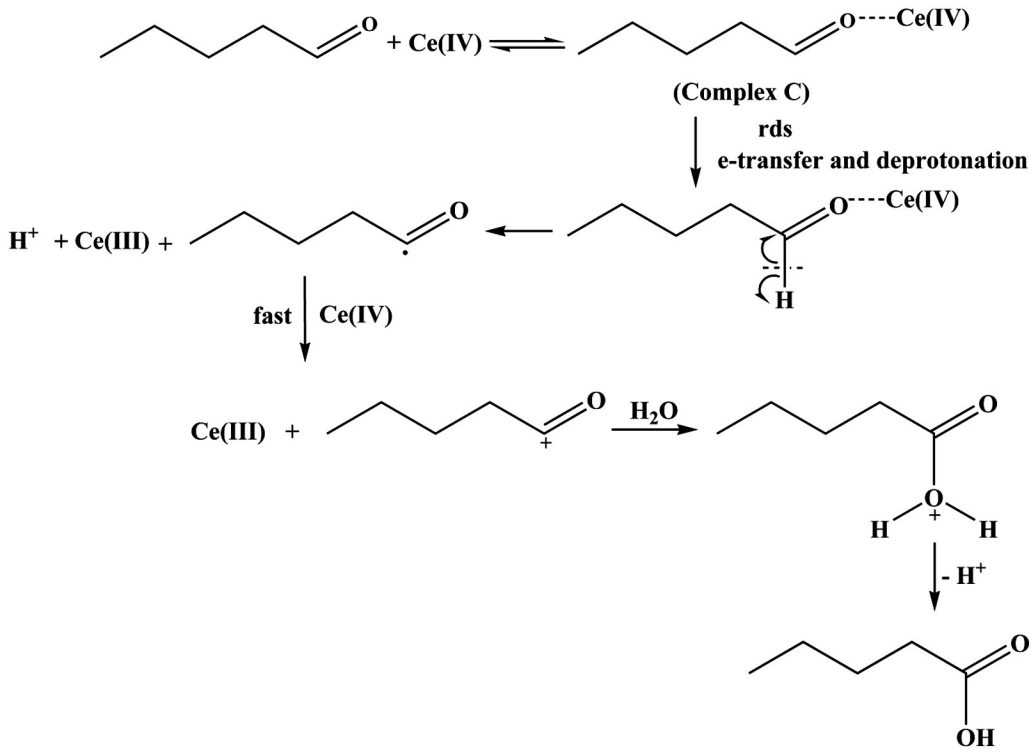

Scheme 1. Oxidation of valeraldehyde in the absence of catalyst by Ce(IV) in aqueous acidic media.

the reactive species $Ce(SO_4)^{2+}$ (presence of positive charge cloud around it) and the substrate aldehyde (presence of electron cloud around on it) come closer to the zwitterionic CHAPS micellar surface (containing a sulfobetaine group), which increases the local molarities in the Stern layer. Addition of metal-salt caused neutralization of micellar surface charge (Scheme 4b), consequently catalyzed the reaction by virtue of increased concentration of reactants in the Stern layer. The head groups of zwitterionic (or amphoteric) detergents are hydrophilic and contain both positive and negative charge in equal numbers, resulting in zero net charge.

From these results in Table 1 it is possible to conclude that the surfactant CHAPS interacts with both anion and cation molecules resulting in electrostatic interaction with reactant and surfactant micelles. The surfactant molecules prefer to micellize with monomer molecules than themselves. It is possible to interpret differences considering that the chemical structure of CHAPS is quite different than the linear hydrocarbon chain of other charged surfactants, therefore one can expect specific interactions between CHAPS and the cationic complex. The specific interactions are an additional contribution to the free energy of mixed micelles aggregation, and in these mixtures, they favor the increment of effective concentration of reactants and thereby increase in the number of collisions between the reactant molecules gives rise to rate enhancement.

4.5.3. Rate enhancement effect by CTAB

CTAB forms reverse micelle (RM) (Scheme 4e and f) which has been found to possess an increased water solubilization capacity compared to other RMs, which is important in the synthesis of nanoparticles, increasing the reactant concentration leading to an increase in the reaction rate. CTAB RMs are frequently utilized, not only because of their confined water core, but also for additional advantages associated with an increased interphase fluidity, leading to greater intermicellar exchange. CTAB requires the presence of a co-surfactant, typically a medium chain hydrophobic organic solvent as in the case of valeraldehyde, in order to form stable RMs. During micellization, valeraldehyde and CTAB molecules were distributed between RM and continuous phases and were

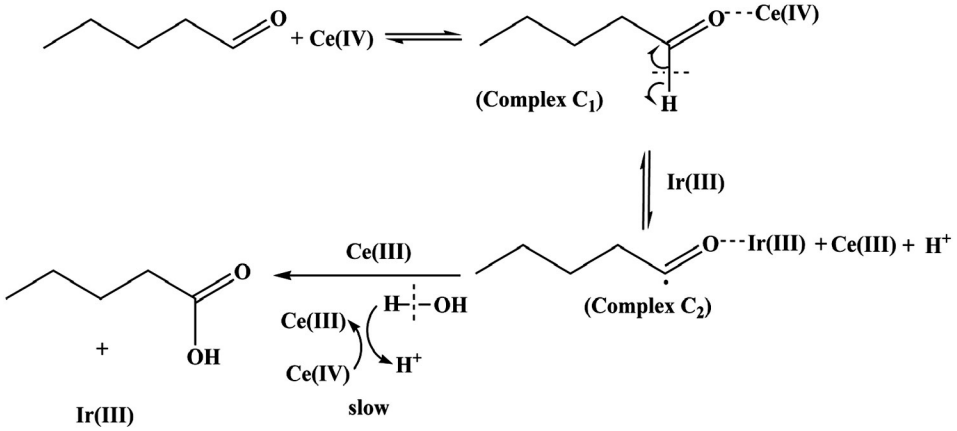

Scheme 2. Oxidation of valeraldehyde in the presence of Ir(III) catalyst by Ce(IV) in aqueous acidic media.

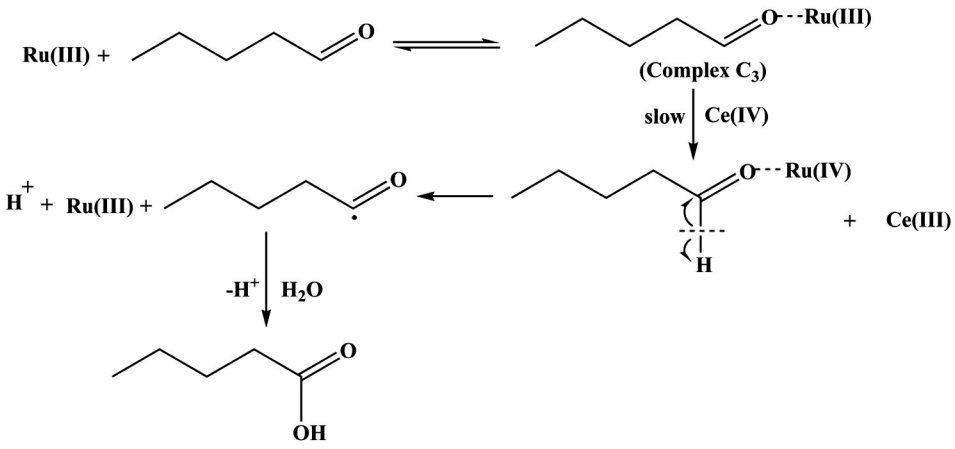

Scheme 3. Oxidation of valeraldehyde in the presence of Ru(III) catalyst by Ce(IV) in aqueous acidic media.

observed to exchange between these two environments. [53]. It was also observed that the reaction rate increases with the CTAB concentration when the surfactant concentration is low and then decreases with further increase in the surfactant concentration. It seems that with increase in the CTAB concentration, different interactions are involved between substrate and surfactants.

Since the charges on the CTAB reverse micelles and Ce(IV) species are same, these studies imply that confinement is more important than surfactant charge for this reaction [54]. The positive catalytic effect of CTAB micelles is most probably due to the formation of reverse micelle during the oxidation of the aldehyde. The reactions in reverse micelles are possible at high concentrations of hydrophobic substrates, and in regard to homogeneous reaction media which can be divided into three spatial domains: the aqueous core, the hydrophilic–hydrophobic interface (Scheme 4e and f), and the surrounding hydrophobic medium [46]. Reverse micelles are nanometer-sized (1–10 nm) water droplets dispersed in organic media obtained by the action of surfactants. Here valeraldehyde acts as organic solvent. This molecule can be solubilized in the water pool of reverse micelles. When surfactants aggregate in non-polar solvents, their polar or charged groups are located in the interior or core of the aggregate while their hydrocarbon tails are extend into the the bulk solvent. Thus water is readily solubilized in the polar core, forming a water pool. When the reactants are in the water pool they are concentrated and act as a nano-reactor leading to concentration effect in the micellar pseudo-phase. Valeraldehyde has an ability to be accommodated more in the palisade layer than in the micellar core due to its large hydrophobic aromatic ring. In the present reaction the oxidation of valeraldehyde by Ce(IV) has been investigated in acidic medium. In this medium the positively charged sulphato-ceric species is the reactive species.

From the rate data (Table 1), it is observed that the reaction is catalyzed marginally in the presence of CTAB when compared to the rate at aqueous medium. In that context the observed rate is found higher compared to the uncatalyzed reaction. So it is expected that the rate constant should increase with increase in [CTAB]. But actually it is observed that next increase in concentration of CTAB in the medium the reaction rate levels off (Fig. 7a). At a certain concentration the effect of CTAB in the rate levels off. This may probably due to the positively charged reactive species of cerium(IV) is repelled by the next incoming positively head groups at the core of the CTAB reverse micelle upon further increase in [CTAB]. It has also been established that micelles can cause the change of mechanism of reactions.

CTAB, which produces cationic micelles ([CTAB] = 1.5×10^{-3} mol dm^{-3}) in aqueous medium, has been found to increase the rate constants (110.3×10^{-6} s^{-1}, Table 1). The $t_{1/2}$ value for the uncatalyzed reaction was found 1.71 h (Table 1) which was reduced to 1.378 h for CTAB ($=1.5 \times 10^{-3}$ mol dm^{-3}) catalyzed reaction. The catalytic activity of CTAB is due to the association of the positively charged species of cerium(IV) on the surface of the cationic micelles. Thus, the mechanism operative in the aqueous medium is also being

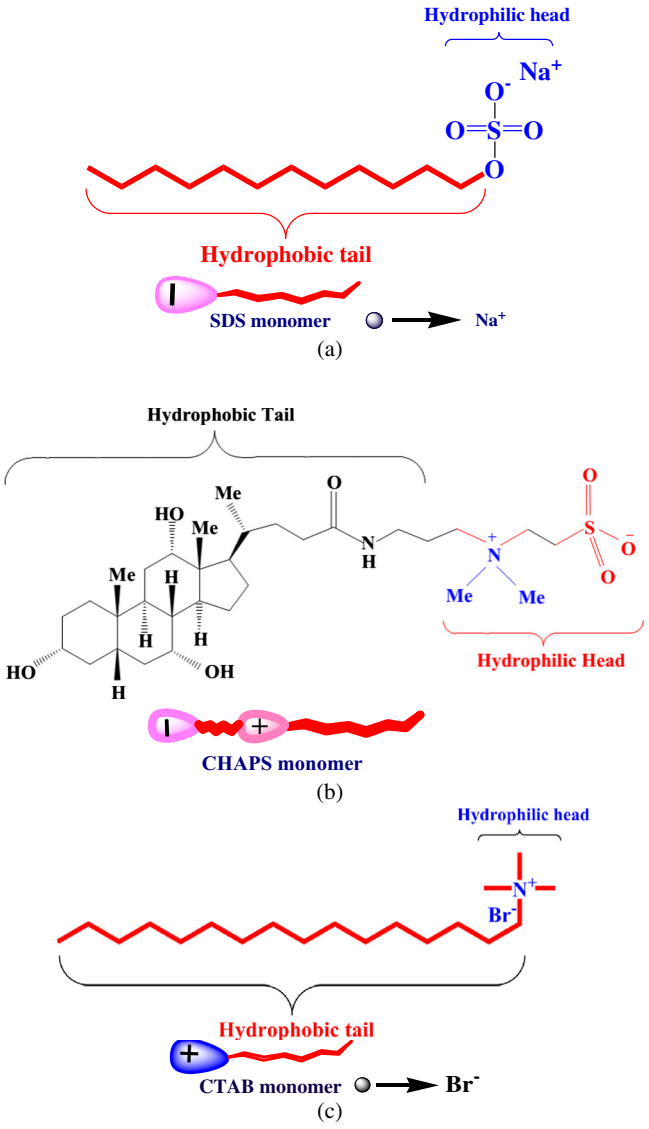

Fig. 9. (a) Molecular structure of surfactant SDS; (b) molecular structure of surfactant CHAPS; (c) molecular structure of surfactant CTAB.

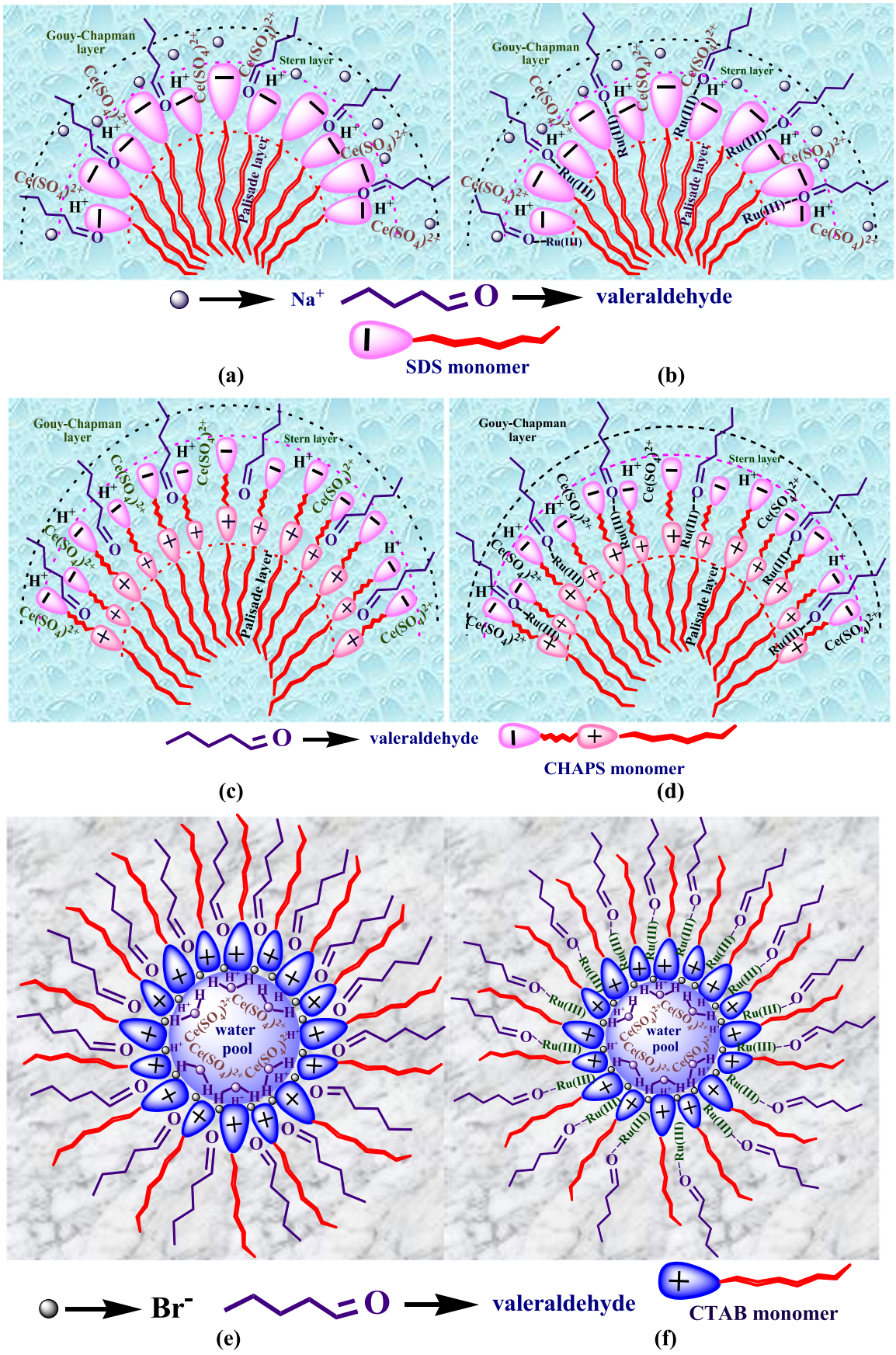

Scheme 4. Schematic model showing probable reaction site for the micellar mediated oxidation reaction between: SDS micelle: (a) [Ce(IV)] species, valeraldehyde and proton; (b) [Ce(IV)] species, Ru(III)-valeraldehyde and proton;. CHAPS micelle: (c) [Ce(IV)] species, valeraldehyde and proton; (d) [Ce(IV)] species, Ru(III)-valeraldehyde and proton; and CTAB micelle: (e) [Ce(IV)] species, valeraldehyde and proton; (f) [Ce(IV)] species, Ru(III)-valeraldehyde and proton.

followed in the CTAB micellar medium too. As the reaction proceeds through the formation of a complex, associated Ce(IV) may form **Complex C** (Schemes 1, 4e) with the substrate. The complex, having positive charge, may now orient in a manner suitable for continuing the reaction [34]. CTAB forms reverse micelle (water-in-oil micelle) in which the hydrophilic groups of surfactant are sequestered in the micelle core and the hydrophobic groups extend away from the center. It seems that with increase in the surfactant concentration, different interactions are involved between substrate, main reactive oxidant species [$Ce(SO_4)^{2+}$] and surfactants. On the other hand, surfactant chain length can affect its interaction with substrates. The surfactant charge significantly affected the rate of the complex formation followed by decomposition reaction with CTAB stabilized reactions [55] in almost non polar solvent valeraldehyde showing considerably faster rates than that in water. It can be speculated that these results may reflect the partitioning effects on the reactants located in the water pool gives rise higher reaction rates in the reverse micelles. The CTAB reverse micelle environment in presence of small amount metal catalyst show significant enhancement.

When Ru(III)-substrate complex can incorporate into the water pool of CTAB micelle producing the enhanced rate with an approximately 350-fold. The electron transfer reaction in this complex displays dramatic sensitivity towards reaction with the active species of cerium(IV) in the environment.

As expected, anionic (SDS) and zwitterionic (CHAPS) micelles accelerate reactions of organic substrates with cationic reactive species and other nucleophilic anions, this behavior was often described as "micellar catalysis", and cationic micelles (CTAB) inhibited these reactions. But in our study there was typically rate acceleration effect at CTAB surfactant concentrations just above the cmc, but above the cmc both reactants could not bind to the reverse micelles, and for reactions rate constants decreased gradually. The reaction rate in CTAB reverse micelle is, however, faster than that in plain water. Generally normal micelles are approximately spherical with the head groups in contact with water. With higher surfactant concentration micelles grow and become rod-like, especially in salt solutions. Micelles in water have a hydrocarbon-like interior, with ionic head groups and counter-ions in the Stern layer at the surface in contact with water and ions are oriented around the micelle in the Gouy–Chapman layer (Scheme 4a–d).

In the CTAB micelle, the kinetic and spectroscopic data supports the location of reactants to be in the Stern/palisade layer and water pool having confinement effects on ions in reverse micelles. Interface charge and confinement increased the electron transfer rate between a substrate–catalyst complex and cerium(IV) ion in CTAB reverse micelles compared to aqueous solution. These studies imply that confinement is more important than surfactant charge for this reaction [54].

When surfactant concentration is below CMC, the reaction system is a suspension (under stirring) with two phases, and the reaction rate is very slow. Valeraldehyde was solubilized into the micelles after reaching the surfactant concentration above CMC. Above CMC, the number of micelles increased with the increasing surfactant concentration, so the rate of valeraldehyde oxidation reaction speeded up and a higher conversion was obtained. Further increase of the surfactant concentration induced micelles to expand, which in turn caused slow increase of oil/water interfacial area. It is observed that the rate constant increases in presence of [CTAB], SDS, and CHAPS. The alteration of electron transfer rate constant in the presence of SDS, CTAB, and CHAPS has been investigated at 303 K. The conclusion is that the micellar effects on the electron transfer rate constant can be explained by considering the micelles as a special background electrolyte with a high electric charge and a strong power of hydration [24].

4.6. Effect of metal ion in presence of surfactants

It is evident that SDS and CHAPS produce rate increasing effect both in the presence and absence of metal ions in the entire range of its concentration used, whereas CTAB increases the rate upto the CMC, after that rate is continuously decreasing. The results (Table 1) indicate incorporation/association of the reactants into or at the water pool of cationic CTAB micelles. In case of further excess of CTAB concentration, there is a repulsion between the cationic head-group $NR_3^1R^2(+)$ and the reactive Ce(IV) species, whereas the latter may form an ion pair with the positive head group of SDS and CHAPS micelles, and thus, an increase in the effective concentration of cerium(IV) within a small volume takes place. The pseudo-first-order rate constants of the oxidation reaction between Ce(IV) and valeraldehyde in micellar medium in absence of metal ion vary in magnitude in the order of $\boldsymbol{k_{(SDS)} > k_{(CTAB)} > k_{(CHAPS)} > k_{(Aqueous)}}$. The rate constants for Ru(III)-salt mediated different micellar catalyzed reactions vary in magnitude in the order of $k_{(CTAB)} > k_{(CHAPS)} > k_{(SDS)} > k_{(Aqueous)}$ with the remarkable ~330 fold rate enhancement (Table 1) as compared to that of uncatalyzed reaction. With the help of several kinetic experimental findings it is to worth mentioned that the pseudo-first-order rate constant (k_{obs}) obtained for the uncatalyzed reaction is $1.121 \times 10^{-4}\ s^{-1}$, which has been increased upto small extent in presence of Ir(III) and Ru(III) metal ion. This suggests significant complex formation between metal ions with valeraldehyde in the transition state of the oxidation. But rate constant becomes high when catalytic amount of Ir(III) or Ru(III) is present with the surfactants. Furthermore the rate constants calculated for only SDS, CHAPS and CTAB catalyzed paths are 2.112×10^{-4}, 1.225×10^{-4} and $1.396 \times 10^{-4}\ s^{-1}$ respectively. Interestingly the rate constant found for Ru(III) (6×10^{-4} mol dm^{-3}) mediated CTAB (1.5×10^{-3} mol dm^{-3}) micelle catalyzed pathway is $365.3 \times 10^{-4}\ s^{-1}$, indicate that a dramatic ~330 fold rate enhancement of reaction. From the half life value ($t_{1/2}$) surprisingly when the uncatalyzed reaction undergoes completion at 5.25 h, in presence of Ru(III) metal and CTAB micelle it completes just at 57 s. The main aspect of the metal ion mediated micellar catalysis is the low water content of the by CTAB reverse micelles and the effects that a large amount of substrates may have in the micellar interface. The metal–substrate complex can make effective collision with the positive reactive species of cerium and enhancement of rate is produced. Such enhanced local concentration of reactants increases the observed rate of reaction to a remarkable extent. As it is evident from the $t_{1/2}$ value for the uncatalyzed reaction was found 1.71 h (Table 1) which was gradually reducing in CTAB catalyzed oxidation path in presence of Ir(III) and Ru(III) ion.

The overall analysis of oxidation of valeraldehyde throughout the experiment has been compared to the earlier literature works as presented in Table 2.

4.7. Reactive species of cerium(IV)

From a kinetic point of view, the existence of various cerium(IV) complexes implies serious difficulties for the identification of the actual reacting complex involved in the oxidation process. It was reported that Ce(IV) exists in aqueous sulfuric acid in several forms, and the reactive species depends on the substrate. Our results suggest that the reactive species in this work is $Ce(SO_4)^{2+}$ which is in agreement with the experimental findings and reverse behavior of CTAB micelle [57].

$$Ce^{3+} + SO_4^{2-} \rightleftharpoons Ce(SO_4)^{+} \qquad K_1' = 43 \tag{1}$$

$$Ce(SO_4)^{+} + SO_4^{2-} \rightleftharpoons Ce(SO_4)_2^{-} \qquad K_2' = 5 \tag{2}$$

$$Ce(SO_4)_2^{-} + SO_4^{2-} \rightleftharpoons Ce(SO_4)_3^{3-} \qquad K_2' = 5.5 \tag{3}$$

$$Ce^{4+} + HSO_4^{-} \rightleftharpoons Ce(SO_4)^{2+} + H^{+} \qquad K_1' = 3500 \tag{4}$$

Table 2
A comparative result for oxidation of valeraldehyde using different catalysts.

Entry	Catalyst	[Ref.]	Conditions	Rate constant	half life ($t_{1/2}$)
1.	–	[56]	$[Valeraldehyde]_T = (3–5) \times 10^{14}$ molecules cm^{-3}, chlorine atoms $= (1.8 \times 10^{15})$ molecules cm^{-3}, pressure = 800 Torr, T = 298 K, Pulsed laser photolysis-laser induced fluorescence	2.31×10^{-10} cm^3 $molecule^{-1}$ s^{-1}	–
2.	Solvent = n-heptane	[30]	$[Valeraldehyde]_T = (0.7–27.0) \times 10^{-2}$ mol L^{-1}, $[ClO_2] = (0.5–1.2) \times 10^{-3}$ mol L^{-1},T = 303 K.	11×10^{-4} L mol^{-1} s^{-1}	–
3.	Solvent = Ethyl acetate	[30]	$[Valeraldehyde]_T = (0.7–27.0) \times 10^{-2}$ mol L^{-1}, $[ClO_2] = (0.5–1.2) \times 10^{-3}$ mol L^{-1},T = 303 K.	13.8×10^{-4} L mol^{-1} s^{-1}	–
4	Solvent = MeCN	[30]	$[Valeraldehyde]_T = (0.7–27.0) \times 10^{-2}$ mol L^{-1}, $[ClO_2] = (0.5–1.2) \times 10^{-3}$ mol L^{-1},T = 303 K.	13.3×10^{-4} L mol^{-1} s^{-1}	–
5.	–	[4]	$[Valeraldehyde]_T = 1.0 \times 10^{-2}$ mol dm^{-3}, $[QDC] = 1.0 \times 10^{-3}$ mol dm^{-3}, $[H_2SO_4] = 0.5$ mol dm^{-3}, T = 313 K.	0.91×10^{-4} s^{-1}	2.11 h
6.	Polymer incarcerated Au nanoparticles (PI-Au) = 5 mg	[3]	$[Valeraldehyde]_T = 0.5$ mL, $[Ce(IV)] = 2.0 \times 10^{-4}$ mol dm^{-3}, Toluene 0.5 mL, TEMPO = 100 ppm, P = 1 atm, T = 50 °C.	–	–
7.	$[CHAPS]_T = 10 \times 10^{-3}$ mol dm^{-3}, $[Ru(III)]_T = 6 \times 10^{-3}$ mol dm^{-3}	Our work	$[Valeraldehyde]_T = 2 \times 10^{-3}$ mol dm^{-3}, $[Ce(IV)] = 2 \times 10^{-4}$ mol dm^{-3}, $[CHAPS] = 10 \times 10^{-3}$ mol dm^{-3}, $[Ru(III)] = 2 \times 10^{-6}$ mol dm^{-3}, $[H_2SO_4] = 0.5$ mol dm^{-3}, $\mu = [H_2SO_4–Na_2SO_4] = 2.0$ mol dm^{-3}, T = 30 °C.	264.8×10^{-4} s^{-1}	1.30 min (time of completion)
8.	$[CTAB]_T = 1.5 \times 10^{-3}$ mol dm^{-3}, $[Ru(III)]_T = 6 \times 10^{-3}$ mol dm^{-3}	Our work	$[Valeraldehyde]_T = 2 \times 10^{-3}$ mol dm^{-3}, $[Ce(IV)] = 2 \times 10^{-4}$ mol dm^{-3}, $[CTAB] = 1.5 \times 10^{-3}$ mol dm^{-3}, $[Ru(III)] = 2 \times 10^{-6}$ mol dm^{-3}, $[H_2SO_4] = 0.5$ mol dm^{-3}, $\mu = [H_2SO_4–Na_2SO_4] = 2.0$ mol dm^{-3}, T = 30 °C.	365.3×10^{-4} s^{-1}	56.9 s. (time of completion)

Here, MeCN = Acetonitrile, QDC = Quinolinium dichromate, TEMPO = 2,2′,6,6′-tetramethylpiperidine *N*-oxyl.

$$Ce(SO_4)_2^{2+} + HSO_4^- \rightleftharpoons Ce(SO_4)_2 + H^+ \quad K_2' = 200 \tag{5}$$

$$Ce(SO_4)_2 + SO_4^{2-} \rightleftharpoons Ce(SO_4)_3^{3-} + H^+ \quad K_2' = 20 \tag{6}$$

$$HSO_4^- \rightleftharpoons SO_4^{2-} + H^+ \tag{7}$$

The active kinetic species of the oxidant was found to be $Ce(SO_4)^{2+}$ based on the effect of ionic strength and sulfate ion on the rate of the reaction. It was reported that Ce(IV) exists in aqueous sulfuric acid in several forms, such as Ce^{+4}, $Ce(SO_4)^{2+}$, $Ce(SO_4)_2$, $Ce(SO_4)_3$, $HCe(SO_4)_3^-$; $HCe(SO_4)_4^{3-}$; $H_2Ce(SO_4)_4^{2-}$; $H3Ce(SO_4)_4^-$ and $H4Ce(SO_4)_4$ and the reactive species depends on the substrate. Our results suggest that the reactive species in this work is $Ce(SO_4)^{+2}$ which is in agreement with the results reported so far [20,34,57].

To confirm this finding, several kinetic runs were performed by varying concentration of CTAB micelle in the reaction mixture with keeping all other conditions fixed. The gradual diminishing values of k_{obs} after certain concentration of CTAB were obtained due to the repulsion of positively charged species $Ce(SO_4)^{2+}$ by positively charged head group of CTAB micelle [34].

In the present case, the catalytic role over a concentration range and thereby rate retardation effect above CMC by CTAB micelles clearly suggests the involvement of a postively charged species of cerium (IV). The conformational relaxation rate decreases slightly in the CTAB micelle but is, greatly hindered in the water pool formed by the CTAB reverse micelles with high numbers in medium which continuously repel the subsequent approaching of cationic reactant species. It completely excludes the possibility of $HCe(SO_4)_3^-$, and $H_3Ce(SO_4)_4^-$ being the reactive species. Interaction of surfactant molecules with substrates can result in decreasing or increasing the reaction rate or changing the yield of reaction and sometimes these surfactant molecules acts as reactants [24]. Thus, we may safely conclude that $Ce(SO_4)^{2+}$, might be considered to be the most active species in the present system.

5. Conclusion

We have analyzed the effect of the charged head groups of different surfactants on the interactions between substrate and positive complex. We also illustrated the possible kinetically active species of Ce(IV) by using three different charged surfactant molecules with different electric charge along with electrostatic attraction or repulsion. Remarkable success in enhancing reaction rates has been achieved by applying micelles as catalysts (introducing catalytic moieties in micelle forming surfactants) and by micelle-assisted catalysis. A variety of ruthenium complexes are found to be reactive as well as highly selective catalysts for the oxidation of alcohols, alkenes and aldehydes by Ce(IV) in water as green solvent. Experimental results and molecular modeling suggest that CTAB forms reverse micelle whereas SDS and CHAPS forms normal micelles. In this experiments in molecular catalysis within micelles have been described, focusing on the different interaction of this kind of catalysis that has proven suitable for almost all classes of chemical transformations, ranging from the use of metal ion catalysts. Well-defined core-shell structures can be successfully designed throughout the kinetics of the oxidation. Such nanoreactors behaved as reverse micelles and demonstrated an ability to extract various hydrophilic reactants from water into an organic, apolar environment.

During oxidation of valeraldehyde a drastic ~330 fold enhancement of rate occurs for Ru(III) in association with and CTAB surfactant molecules come to play simultaneously.

Reversibility is another important feature in catalysis to implement control over catalytic activity and catalyst recovery. It is therefore advisable that in the near future recovery of the surfactant or separation of the catalytic system from the reaction mixture would be feasible using this approach.

Acknowledgments

Thanks to UGC, New Delhi and CSIR, New Delhi for providing financial help in the form of a project and fellowship.

Appendix A. Supplementary data

Supplementary data to this article can be found online at http://dx.doi.org/10.1016/j.molliq.2015.06.056.

References

[1] E. Iwasaki, T. Nakayama, Y. Matsumi, K. Takahashi, T.J. Wallington, M.D. Hurley, E.W. Kaiser, J. Phys. Chem. A 112 (2008) 1741–1746.
[2] H.J. Chacon-Madrid, A.A. Presto, N.M. Donahue, Phys. Chem. Chem. Phys. 12 (2010) 13975–13982.
[3] M. Conte, H. Miyamura, S. Kobayashi, V. Chechik, Chem. Commun. 46 (2010) 145–147.
[4] G.S. Chaubey, S. Das, M.K. Mahanti, Croat. Chem. Acta 76 (2003) 287–291.
[5] Campbell, Princess, Science Assessment for Valeric Acid, U.S. Environmental Protection Agency, Office of Prevention, Pesticides and Toxic Substances, Washington, D.C., June 1, 2005, page 3.
[6] Bizzari, Sebastian N., Blagoev, Milen, Kishi, Akihiro, "Oxo Chemicals", CEH Marketing Research Report: Chemical Economics Handbook, SRI Consulting, September 2006, pages 17, 19, and 55.
[7] P. Heymanns, H. Bahrmann, C.D. Frohning, H. Kalbfell, P. Lappe, D. Peters, E. Wiebus, J. Mol. Catal. A Chem. 116 (1997) 35–37.
[8] G.L. Sorella, G. Strukul, A. Scarso, Green Chem. 17 (2015) 644–683.
[9] R. Saha, I. Saha, R. Nandi, A. Ghosh, A. Basu, S.K. Ghosh, B. Saha, Can. J. Chem. Eng. 91 (2013) 814–821.
[10] R. Saha, B. Saha, Desalin. Water Treat. 52 (2014) 1928–1936.
[11] B. Saha, C. Orvig, Coord. Chem. Rev. 254 (2010) 2959–2972.
[12] A. Basu, D. Saha, R. Saha, T. Ghosh, B. Saha, Res. Chem. Intermed. 40 (2014) 447–485.
[13] M. K.-ud-Din, S. Ali, Z. Khan, Colloid Polym. Sci. 285 (2007) 745–752.
[14] F. Khan, U. Kushwaha, A.K. Singh, J. Chem. Pharm. Res. 4 (2012) 3715–3726.
[15] U. Kushwaha, A.K. Singh, A. Singh, Asian J. Chem. 24 (2012) 2373–2376.
[16] P.K. Tandon, M. Purwar, P.B. Dwivedi, M. Srivastava, Transition Met. Chem. 33 (2008) 791–795.
[17] A.K. Das, Coord. Chem. Rev. 213 (2001) 307–325.
[18] S.K. Mondal, D. Kar, M. Das, A.K. Das, Transition Met. Chem. 23 (1998) 593–597.
[19] B. Naskar, S. Ghosh, S. Nagadome, G. Sugihara, S.P. Moulik, Langmuir 27 (2011) 9148–9159.
[20] A. Ghosh, R. Saha, B. Saha, J. Mol. Liq. 196 (2014) 223–237.
[21] S.K. Ghosh, A. Ghosh, R. Saha, B. Saha, Phys. Chem. Liq. 53 (2015) 146–161.
[22] R. Saha, A. Ghosh, B. Saha, Spectrochim. Acta A 124 (2014) 130–137.
[23] K. Mukherjee, A. Ghosh, R. Saha, P. Sar, S. Malik, B. Saha, Spectrochim. Acta A 122 (2014) 204–208.
[24] B. Samiey, C.-H. Cheng, J. Wu, J. Chem. (2014)http://dx.doi.org/10.1155/2014/908476.
[25] T. Sumathi, P. Shanmugasundaram, G. Chandramohan, Arab. J. Chem. 4 (2011) 427–435.
[26] T. Sumathi, P. Shanmugasundaram, G. Chandramohan, J. Saudi Chem. Soc. 17 (2013) 227–235.
[27] P. Sar, A. Ghosh, B. Saha. Res. Chem. Intermed. (DOI http://dx.doi.org/10.1007/s11164-014-1858-4).
[28] K. Mukherjee, B. Saha, Tenside Surftants Deterg. (2015) (in press).
[29] M. Singh, Synth. React. Inorg. Met.-Org. Nano-Met. Chem. 42 (2012) 1315–1326.
[30] E.S. Ganieva, I.M. Ganiev, S.A. Grabovskiy, N.N. Kabalnova, Russ. Chem. Bull. 57 (2008) 2332–2334.
[31] A. Ghosh, R. Saha, B. Saha, J. Ind. Eng. Chem. 20 (2014) 345–355.
[32] R. Saha, A. Ghosh, B. Saha, Chem. Eng. Sci. 99 (2013) 23–27.
[33] V. Briois, D. Lu1tzenkirchen-Hecht, F. Villain, E. Fonda, S. Belin, B. Griesebock, R. Frahm, J. Phys. Chem. A 109 (2005) 320–329.
[34] A. Ghosh, R. Saha, K. Mukherjee, P. Sar, S.K. Ghosh, S. Malik, S.S. Bhattacharyya, B. Saha, J. Mol. Liq. 190 (2014) 81–93.
[35] M. Martos, B.J. López, J.V. Folgado, E. Cordoncillo, P. Escribano, Eur. J. Inorg. Chem. 2008 (2008) 3163–3317.
[36] M. Jabbari, F. Gharib, Monatsh. Chem. 143 (2012) 997–1004.
[37] Y. Zhai, H. Liu, B. Liu, Y. Liu, J. Xiao, W. Bai, Transition Met. Chem. 32 (2007) 570–575.
[38] B. Hernawan, T. Purwono, D. Wahyunngsih, Int. J. Eng. Technol. IJET-IJENS 12 (2012) 1–4.
[39] F.P. Cavasino, R. Cervellati, Renato Lombardo, M.L.T. Liverifor, J. Phys. Chem. B 103 (1999) 4285–4291.
[40] A. Ghosh, R. Saha, P. Sar, B. Saha, J. Mol. Liq. 186 (2013) 122–130.
[41] M.K. Ghosh, S.K. Rajput, Int. Res. J. Pure Appl. Chem. 3 (2013) 308–319.
[42] P.K. Tandon, S. Sahgal, A.K. Singh, S. Kumar, M. Dhusia, J. Mol. Catal. A Chem. 258 (2006) 320–326.
[43] Z. Hu, H. Du, C. Fai Leung, H. Liang, Tai-Chu Lau, Ind. Eng. Chem. Res. 50 (2011) 12288–12292.
[44] K. Karunakaran, K.P. Elango, React. Kinet. Catal. Lett. 62 (1997) 353–358.
[45] R. Saha, A. Ghosh, P. Sar, I. Saha, S.K. Ghosh, K. Mukherjee, B. Saha, Spectrochim. Acta A 116 (2013) 524–531.
[46] T. Dwars, E. Paetzold, G. Oehme, Angew. Chem. Int. Ed. 44 (2005) 7174–7199.
[47] N.J. Buurma, J. Adv. Phys. Org. Chem. 43 (2009) 1–37.
[48] L. Onel, N.J. Buurma, J. Phys. Chem. B 115 (2011) 13199–13211.
[49] C. A. Bunton, ARKIVOC 2011 (vii) 490–504.
[50] K. ud-Din, M.S. Ali, Z. Khan, Acta Phys. -Chim. Sin. 24 (2008) 810–816.
[51] L. García-Rio, J.C. Mejuto, M. Pérez-Lorenzo, J. Colloid Interface Sci. 301 (2006) 624–630.
[52] S. Zhaoa, X. Wanga, M. Huo, Appl. Catal. B Environ. 97 (2010) 127–134.
[53] A.J. Mills, J. Wilkie, M.M. Britton, J. Phys. Chem. B 118 (2014) 10767–10775.
[54] E. Gaidamauskas, D.P. Cleaver, P.B. Chatterjee, D.C. Crans, Langmuir 26 (2010) 13153–13161.
[55] N.M. Correa, J.J. Silber, R.E. Riter, N.E. Levinger, Chem. Rev. 112 (2012) 4569–4602.
[56] S. Singh, S. Herandez, Y. Ibarra, A.S. Hasson, Int. J. Chem. Kinet. 41 (2009) 133–141.
[57] M. Hassan, M.D. AlAhmadi, M. Mosaid, Arab. J. Chem. 8 (2015) 72–77.